Simulating the performance of the Pong Reservoir in India under climate change perturbations

Simulating the Performance of the Pong Reservoir in India under Climate Change Perturbations

Bankaru-Swamy Soundharajan [1], **Adebayo J. Adeloye** [1]*****, **Renji Remesan** [2] **and C. S. P. Ojha** [3]

[1] School of the Built Environment, Heriot-Watt University, Edinburgh, United Kingdom
[2] Cranfield University, Cranfield, UK
[3] Indian Institute of Technology Roorkee, India
(*Corresponding author: E-mail: *a.j.adeloye@hw.ac.uk)*

Abstract
This paper assessed the implications of plausible climate change perturbations on the performance characteristics of the Pong Reservoir on the Beas River, Himachal Pradesh, India. Simulated historic and climate-change runoff series developed using the HYSIM rainfall-runoff model of the snowy catchment, formed the basis of the analysis. The climate perturbations used delta changes in temperature (from 0°C to +2°C) and precipitation (from -10% to +10% of annual rainfall). Reservoir simulations were then carried out, forced with the simulated runoff records, guided by rule curves derived by a coupled sequent peak algorithm and genetic algorithm optimiser. The resulting performance was summarised in terms of reliability, resilience, vulnerability and sustainability. The results show that when the runoff increases in the future due to higher rainfall, the performance of the reservoir will improve. Of notable importance is the vulnerability or water shortfall, which more than halved for a 5% increase in rainfall and completely disappears if the rainfall increases by 10%. Decreases in the rainfall produced the opposite effect, i.e. caused the vulnerability to worsen. Increases in the temperature (and the additional runoff generated from snowmelt) appeared to partially annul the effect of reduced rainfall on the runoff causing the performance of the reservoir to improve as the temperature rises. Ways of ameliorating the water shortage difficulties are suggested, including better operational practices that manage the available water through hedging.

Keywords
Reservoir operation, rule curves, genetic algorithm, Pong Reservoir, India

1. INTRODUCTION

Effective Reservoir operation is important to accommodate the inevitable differences between the hydrology used for reservoir planning and the prevailing hydrology when operating the reservoir. Climate change is predicted to affect the hydrology of most regions through its influence on temperature, rainfall, evapotranspiration, etc., which may further the divergence between the planning and operational hydrological situations. The Pong dam reservoir on the Beas River (Figure 1) is multi-purpose, serving both hydropower and irrigation water needs

(Jain et al., 2007). Its inflow is highly influenced by both the Monsoon rainfall and the melting snow from the Himalayas; consequently, its ability in satisfactorily performing its functions is susceptible to possible disturbances in these climatic attributes due to climate change. For a system that is inextricably linked to the socio-economic well being of its region, any significant deterioration in performance or ability to meet the demand will have far reaching consequences. This is why it is important to carry out a systematic assessment of the performance of the reservoir during climate change and to use the outcome to inform the development of appropriate solutions.

The Pong, like most reservoirs, is operated using rule curves, which guide the operator's decision on the quantity of water to release based on the available water in the reservoir at the beginning of each month. Because currently used curves were not made available, new rule curves were derived as part of the current study using the Sequent Peak Algorithm, SPA (McMahon and Adeloye, 2005). Further refinement of the SPA-derived rule curves was achieved through genetic algorithms (GA) optimisation, with the SPA-derived curves defining the limits for the random sampling of the GA initial solution population. The rule curves derived via the coupled SPA-GA approach then formed the basis of further reservoir simulations to derive performance indices for the Pong when forced with different simulated runoff scenarios, including the climate-change perturbed runoff.

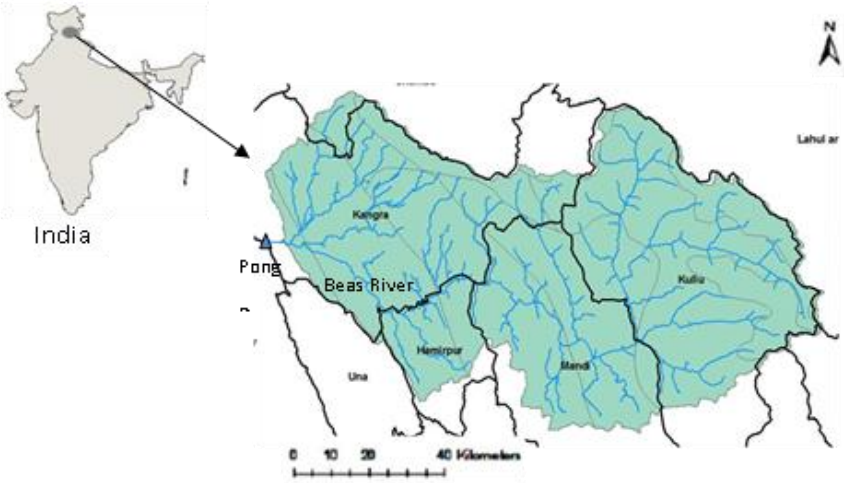

Fig. 1 Map of India and the Beas river catchment

The climate change perturbation used a scenario-neutral, delta approach to remove the inevitable uncertainties associated with the use of GCM-derived/downscaled scenarios. On the other hand, such delta perturbations are quite efficient in identifying tipping points at which the reservoir is likely to fail catastrophically in

meeting water demand. In the next Section, further details about the adopted methodology are provided. This is followed by a description of the Case study catchment and the data used. The results are then presented and discussed, followed by the main conclusions of the study.

2. METHODOLOGY

2.1. HYSIM rainfall-runoff modelling

A conceptual overview of the HYSIM rainfall-runoff model is shown in Figure 2.

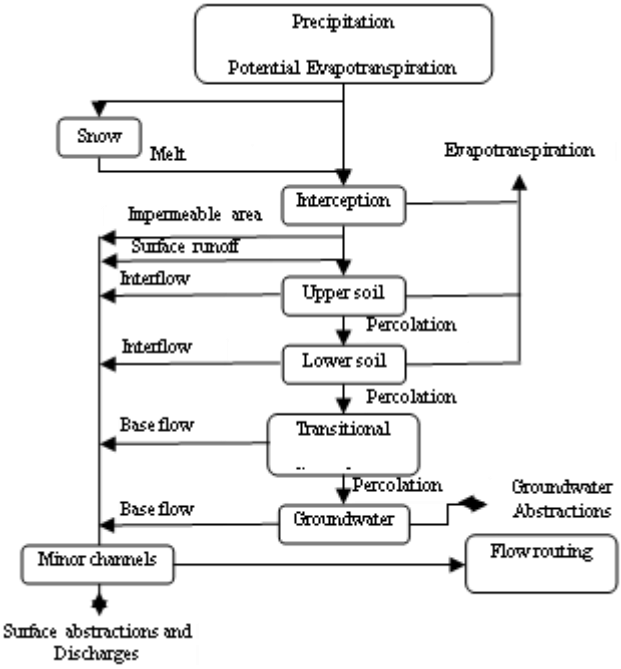

Fig. 2 The schematic diagram of HYSIM model

HYSIM is a time-continuous, conceptual rainfall-runoff model that has been successfully used in various situations, including snowy catchments similar to the Beas (see Pilling and Jones, 1999; Murphy et al., 2006). As conceptualised in Figure 2, the model has two sub-routines simulating respectively the river basin hydrology and the channel hydraulics. Main inputs are the precipitation and potential evapotranspiration; if data on the latter are unavailable, they can be derived using one of the available empirical/theoretical approaches, e.g. the Penman-Monteith (Adeloye et al., 2011). HYSIM has several parameters as detailed by Pilling and Jones (1999); the initialisation of these parameters in this study relied on Harmonized World Soil Database (HWSD) analysis and were then modified during the calibration of the model.

2.2. Rule Curves derivation

A coupled SPA-GA approach was used to derive and optimise the upper and lower rule curves for the Pong. The SPA obtains reservoir storage capacity using sequential deficits over an N-month period as follows (McMahon and Adeloye, 2005):

$$K_{t+1} = \max(0, K_t + D_t - Q_t); t \in N \quad (1)$$

$$K_a = \max(K_{t+1}) \quad (2)$$

where K_a is the capacity, K_{t+1} and K_t are respectively the sequential deficits at the end and start of time period t, D_t is the demand during t, Q_t is the inflow during t and N is the total number of time periods in the data record. Once the time series of K_t are available, the corresponding reservoir storage can be estimated using:

$$S_t = K_a - K_t \quad (3)$$

Using the time series of S_t, initial estimates of the ordinates of the upper and lower rule curves for each month of the year were obtained using:

$$URC_m = \max(s_{y,m}),\ y = 1, n;\ m = 1, 12 \quad (4)$$

$$LRC_m = \text{average}(s_{y,m}),\ y = 1, n;\ m = 1,12 \quad (5)$$

where URC_m and LRC_m are, respectively, the upper and lower rule curves ordinates for month m, and n (=N/12) is the number of years in the data record. The two dimensional storage variable "s" is related to the one-dimensional storage variable "S" by $s_{y,m} = S_{12(y-1)+m}$, i.e. t = 12(y-1)+m. To refine the SPA-derived rule curves, they were optimised using Genetic Algorithm, GA involving the minimisation of the sum of squares of the water deficit $\left(D_t - D_t^{'}\right)$, i.e.:

$$\text{Minimise } \sum_{i=1}^{N}\left(D_t - D_t^{'}\right)^2;\ t \in N \quad (6)$$

The constraints are as follows:

$$S_{t+1} = S_t + Q_t - D'_t - E_t,$$

$$WA_t = S_t + Q_t$$

$$\text{if } WA_t \geq URC_m,\ D'_t = S_t + Q_t - E_t - URC_m \ \&\ ER_t = D'_t - D_t$$

$$\text{if } URC_m \geq WA_t > LRC_m,\ D'_t = D_t \ \&\ ER_t = 0$$

$$\text{if } WA_t \leq LRC_m,\ D'_t = 0$$

where WA_t is the water available at beginning of time period t; E_t is the reservoir surface net evaporation loss during t; ER_t is excess release during time period t, S_t is the storage at the beginning of t, D'_t is the actual release and all other symbols are as previously defined. The decision variables for the optimisation are the $URCm$ and LRC_m ordinates for each month m of the year (m=1..,12), giving a total of 24

variables. The GA optimisation involved the usual selection, crossover and mutation operations (Hossain and El-shafie, 2013; Wardlaw and Sheriff, 1999). A real-value coding was used with the following parameters: crossover fraction = 0.8; mutation rate = 0.01; number of elite children = 2. The genetic operations were repeated for 500 generations.

2.3. Reservoir simulation and Performance indices

Reservoir simulation used the mass balance equation of the inflows and outflows for the reservoir as follows:

$$S_{t+1} = S_t + Q_t - D'_t - E_t; \qquad LRC_m \le S_{t+1} \le URC_m \quad (7)$$

The results of the simulation were then used to estimate four performance indices as follows (McMahon et al., 2006; Adeloye, 2012):

Reliability: this can be expressed either in the time-domain, R_{elt} or volume domain, R_{elv} as follows:

$$R_{elt} = N_s / N \quad (8)$$

$$R_{elv} = \sum_{t=1}^{N} D'_t \Big/ \sum_{t=1}^{N} D_t \quad (9)$$

where N_s is the total number of intervals out of N that the demand was met.

Resilience: Resilience is a measure of the reservoir's ability to recover from failure and defined as:

$$\varphi = 1/(f_d/f_s) = f_s/f_d; \qquad 0 < \varphi \le 1 \quad (10)$$

where φ is resilience, f_s is number of continuous sequences of failure periods and f_d is the total duration of the failures, i.e. $f_d = N - N_s$.

Vulnerability: The vulnerability, η, is (Sandoval-Solis et al., 2011):

$$\eta = \sum_{t=1}^{f_d} [(D_t - D'_t)/D_t] \Big/ f_d \; ; t \in f_d \quad (11)$$

Sustainability: A sustainability, λ, index that integrates the three earlier defined indices was used (Sandoval-Solis et al., 2011):

$$\lambda = (R_{elt}\varphi(1-\eta))^{1/3} \quad (12)$$

3. CASE STUDY AND DATA

The Beas River, on which the Pong dam is located, is one of the five major rivers of the Indus basin, India. The reservoir, located at longitude 76° 05′ E and latitude 32° 01′ N, drains a catchment area of 12,561 km², out of which the permanent snow catchment is 780 km² (Jain et al., 2007). Active storage capacity of the reservoir is 7051 Mm³. Apart from its use for generating hydropower, the Pong meets irrigation water demands, which are spread relatively uniformly throughout the year (see Figure 3). Monsoon rainfall between July and September is a major source of water inflow into the reservoir, apart from snow and glacier melt. Daily reservoir inflow and release from January 2000 to December 2008 (8 years) were available for the study. The historic mean annual runoff (MAR) at dam site is 8485 Mm³ (annual coefficient of variation is 0.225) and the seasonal distribution of the runoff is also shown in Figure 3.

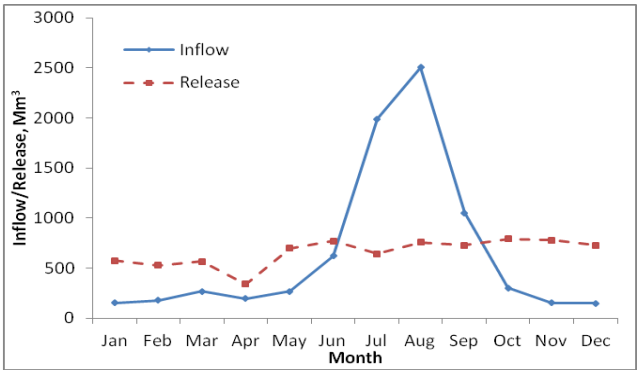

Fig. 3 Average monthly inflow and release from Pong dam (data: 2000-2008)

Gridded TRMM (TRRM 3B42 V7) daily rainfall data that span the runoff period were used for the study. The TRMM data have a fine spatial resolution (0.25 degree * 0.25 degree), covering the latitudinal band of 50° N-S. Since potential evapotranspiration (ETo) measurements were unavailable, estimates were obtained using the Penman-Montheith (P-M) formulation forced with meteorological variables from the NCEP Climate Forecast System Reanalysis (CFSR) data from January 1999 – December 2008. The summary of the rainfall, temperature and the estimated P-M ETo data are shown in Table 1.

Table 1. Summary of the precipitation, ETo and temperature for the Pong catchment

Statistics	Precipitation mm/day	ETo mm/day	Temperature °C		
			Max	Min	mean
Mean	3.40	3.93	20.92	7.98	14.45
Maximum	113.58	9.82	36.25	21.55	28.20
Minimum	0.00	0.46	1.87	-11.71	-1.98
SD	8.22	1.68	6.78	6.53	6.47

4. RESULTS AND DISCUSSION

4.1. Calibration of HYSIM Model

The available data record was split into two: calibration (2000 – 2004) and validation (2005 – 2008). Although HYSIM was implemented on a daily timescale, the results presented here are the monthly summaries to coincide with the time-scale used for the reservoir studies. The monthly performance of the model during calibration and validation is shown in Figure 4 from where it can be seen that the model has performed reasonably well in reproducing the measured runoff.

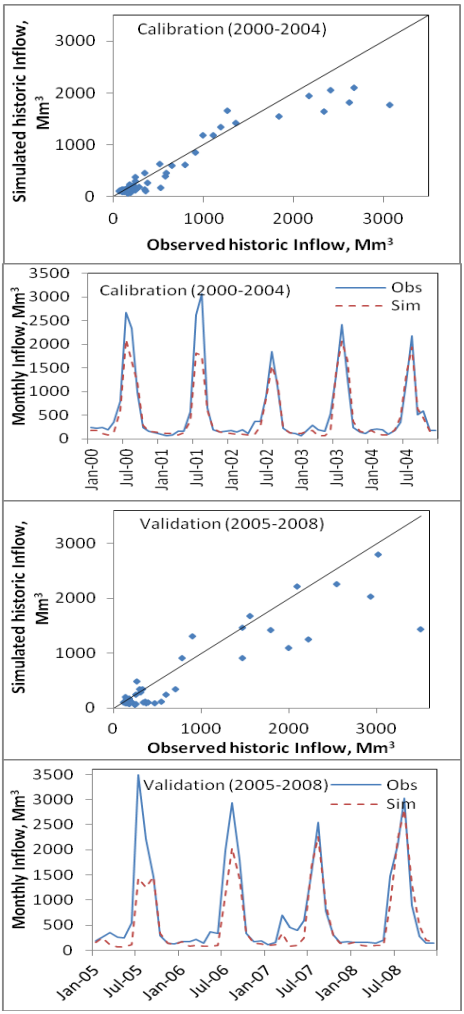

Fig. 4 Comparison of observed and simulated monthly river flow during calibration and validation

More re-assuring is the relatively better performance of the model in simulating the

low runoff sequence in the data, which is more important for water resources planning than the high flows periods. The estimated Nash-Sutcliffe efficiency indices during the calibration and validation were respectively 0.88 and 0.78, both of which lend further credence to the modelling skill of the calibrated HYSIM.

4.2. Climate Change Effects on Reservoir Inflows

With HYSIM satisfactorily validated, it was possible to use the model to assess the impacts of changes in the precipitation and temperature on the runoff. Table 2 summarises the effect of changes in the precipitation and temperature on the simulated annual and seasonal runoff at the Pong. As expected, increasing the precipitation causes the annual runoff to increase and vice versa. However, while increasing or decreasing the precipitation by the same amount has resulted in similar absolute change in the runoff for no change in temperature, the situation is different when temperature increases are considered. For example, as shown in Table 2, while an increase in the annual precipitation of 5% produced a 10.21% increase in the annual runoff if the temperature increased by 1^{o}C, a similar decrease in precipitation with the 1^{o}C temperature increase only resulted in a decrease of only 1.6 % in the annual runoff. As noted previously, the Beas hydrology is heavily influenced by the melting snow from the Himalayas and what these results show is that the runoff contributed by the melting snow partially compensates for the reduction in direct runoff caused by the combined effects of lower precipitation and higher (temperature-induced) evapotranspiration. Indeed, as the assumed temperature increase becomes higher, the effect of any reduction in the annual precipitation fully disappears, resulting in a net increase in the annual runoff. Consequently, increasing the temperature by 2^{o}C has resulted in a net increase in the annual runoff of 12.4% and 7% respectively for 5% and 10% reduction in the annual precipitation.

The annual runoff situation presented above masks the significant seasonal differences in simulated runoff response of the Beas. As Table 2 clearly shows, both the post-Monsoon and winter seasons that do not benefit from the melting snow and its associated runoff tended to be well-behaved in terms of the response, with reductions in the precipitation producing significant reductions in the generated runoff. Indeed, for these two seasons, increasing the temperature can worsen the runoff situation even for situations in which the precipitation has increased, as clearly revealed by the 2.4% reduction in the winter runoff with 1^{o}C and 5% rises, respectively, in the temperature and precipitation. These situations must be resulting from the dominance of the evapotranspiration loss, which in the absence of additional water from melting snow will make the runoff to decrease.

The observed changes in runoff would have implications for the ability of the Pong dam to meet the demand placed on it. However, due to the complex nature of the interactions between inflow, demand, operating policy and other characteristics of a reservoir, it is difficult to infer the resulting performance by merely looking at the runoff situation alone. To do this properly will require simulating the reservoir

using the available operating policy as previously demonstrated by Nawaz and Adeloye (2006). The next section presents the result of the performance evaluation.

Table 2. Mean annual (Mm^3) and Seasonal (Mm^3) Runoff of simulated series (The values in the parenthesis are change (%) of runoff from the simulated historic)

Temperature change, °C	Annual precipitation change, %				
	-10	-5	0	+5	+10
			Annual		
0	5465.08 *(-12.11)*	5829.16 *(-6.25)*	6217.92 *(0.00)*	6634.23 *(6.70)*	7074.11 *(13.77)*
+1	5777.68 *(-7.08)*	6116.36 *(-1.63)*	6476.91 *(4.17)*	6853.01 *(10.21)*	7239.86 *(16.44)*
+2	6652.22 *(6.98)*	6989.75 *(12.41)*	7349.26 *(18.19)*	7726.83 *(24.27)*	8115.11 *(30.51)*
			Season: Winter		
0	355.96	382.36	410.33	442.22	477.62
+1	335.17	354.72	376.74	400.65	425.98
+2	386.14	405.30	426.73	450.35	475.28
			Season: Post-Monsoon		
0	278.29	301.79	327.75	356.87	389.43
+1	269.53	288.25	308.99	331.33	354.92
+2	318.04	337.69	359.54	383.25	408.29
			Season: Monsoon		
0	3366.65	3594.50	3838.36	4098.01	4369.80
+1	3656.26	3877.94	4111.88	4355.69	4607.21
+2	4193.58	4414.34	4647.22	4890.75	5142.03
			Season: Pre-Monsoon		
0	1464.18	1550.51	1641.49	1737.13	1837.26
+1	1516.72	1595.45	1679.30	1765.34	1851.75
+2	1754.47	1832.41	1915.78	2002.47	2089.51

4.3. Simulated Performance of the Pong

The optimized rule curves obtained via GA are shown in Figure 5, on which are superimposed the approximate rule curves developed using the SPA. As noted previously, the SPA curves formed the basis for the initial sampling of the GA solution. The GA used real value coding and each ordinate of the rule curve was assumed to be uniformly distributed, with upper and lower limits defined by:

$$URC = U\left[URC_{m(SPA)} - \sigma_{s_{y,m}}\ ; URC_{m(SPA)} + \sigma_{s_{y,m}}\right]; y = 1,n; m = 1,12 \quad (13)$$

$$LRC = U\left[LRC_{m(SPA)} - \sigma_{\bar{s}_{y,m}}; LRC_{m(SPA)} + \sigma_{\bar{s}_{y,m}}\right]; y = 1,n; m = 1,12 \quad (14)$$

where $U[X;Y]$ is the uniform density function with lower (X) and upper (Y) bounds as specified, $U(L)RC_{m(SPA)}$ is the SPA upper(lower) rule curve ordinate in month m, $\sigma_{s_{y,m}}$ is the standard deviation of reservoir storage during month m and $\sigma_{\bar{s}_{y,m}}$ is the

standard deviation of the mean reservoir storage during month m. In general, $\sigma_{\bar{s}_{y,m}} = \frac{\sigma_{s_{y,m}}}{\sqrt{n}}$, where n is the number of years in the record = 9 (2000 – 2008).

The array of all the performance indices is summarized in Table 3. A quick comparison of R_{elt} and R_{elv} values will reveal that $R_{elv} \geq R_{elt}$ for all the scenarios as expected. Additionally, whenever there are no failures (i.e. $f_s = f_d = 0$), both the vulnerability and resilience are undefined as expected. Thus all the estimated indices are well-behaved. However, for lack of space, further discussion will highlight the vulnerability because, while all the other indices are useful, the vulnerability by characterizing the quantity of shortage is more relevant when considering the impact of water shortage on users.

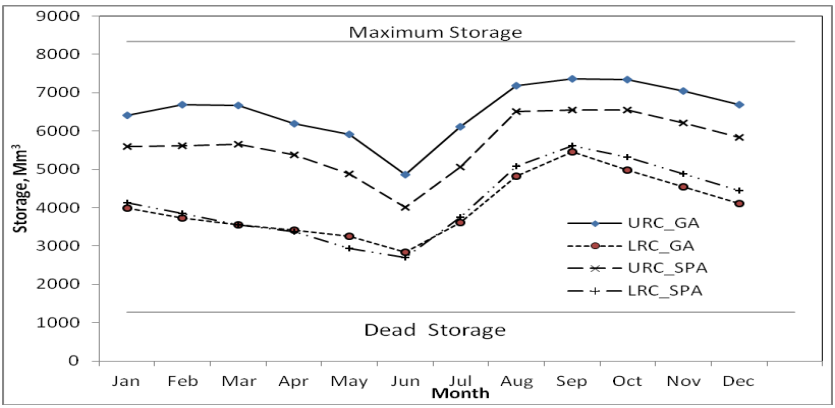

Fig. 5 Rule curves develped by GA and SPA

As shown in Table 3, the historic vulnerability of 0.18 is reduced as the runoff increases but worsened when the runoff reduces if the temperature is unchanged, which is to be expected since more runoff implies more inflows and less shortage. As was the case with the runoff, however, the lower-precipitation induced intensification of the vulnerability is tempered by increases in the temperature because of the indirect effect of the increased temperature on the runoff. Thus, while a reduction of 10% in the precipitation caused the vulnerability to more than double for no change in temperature, the same change in precipitation decreased it to 0.07 for a 2 ^{o}C temperature rise.

The above results would imply that while the Pong is performing satisfactorily in meeting the demand with vulnerability of 18%, there is the possibility that the vulnerability may intensify to almost 40% if the precipitation received by the catchment reduces significantly in a warming climate. As suggested by Fiering (1982), most water users are able to cope with water shortage of up to 25% of that

required but significant consequences can result at shortages above this critical threshold. Therefore, ways must be devised to ameliorate this potential problem. One possibility is to re-design the rule curves for the reservoir, utilizing the future levels of runoff at the catchment. As noted earlier, the current exercise used rule curves optimized for the historic runoff conditions, which may not be appropriate for the future hydrology. A further way by which the problem can be tempered is to adopt a system of hedging for the reservoir, in which water during normal operation of the reservoir is held back so as to meet larger shortages during droughts. Several studies have demonstrated that hedging can reduce the vulnerability by ensuring that shortages are spread evenly instead of the few large, crippling shortages that can result without hedging.

Table 3. Summary of performance indices evaluated in this study using the GA optimised reservoir rule curves

Temperature Change, °C	Precipitation Change, %	Performance Indices				
		R_{elv}	R_{elt}	φ	η	λ
0	-10	0.89	0.78	0.26	0.37	0.5
	-5	0.94	0.86	0.4	0.31	0.62
	0	0.97	0.92	0.37	0.18	0.65
	+5	0.99	0.96	0.25	0.09	0.6
	+10	1	1	-	-	-
+1	-10	0.93	0.85	0.31	0.33	0.56
	-5	0.96	0.88	0.38	0.19	0.65
	0	0.99	0.94	0.5	0.15	0.73
	+5	1	1	-	-	-
	+10	1	1	-	-	-
+2	-10	0.99	0.98	0.5	0.07	0.76
	-5	1	1	-	-	-
	0	1	1	-	-	-
	+5	1	1	-	-	-
	+10	1	1	-	-	-

5. CONCLUSIONS

This study has assessed the impact of plausible changes in the climate on both the inflows and performance of the Pong reservoir in India. The results showed that increasing the precipitation will cause the reservoir inflow to increase while decreasing it will result in the opposite effect. However, if the changes in precipitation are accompanied by increases in the temperature, the effect of decreases in precipitation is somewhat tempered due to the additional runoff generated by melting snow with the rise in temperature. This shows the buffering effect of the snow on this catchment, which may be lost if projected climate change results in the depletion of the snow cap in the Himalayas where the catchment is situated. Further simulation studies of the reservoir performance produced results that largely agree with the obtained trend in the runoff. In particular, it was found that the vulnerability or water shortage will be worse as the available inflow into the reservoir decreases. This calls for better ways of managing and operating the

Pong if the predicted climate change holds, including re-designing the rule curves using the anticipated future runoff and the integration of hedging into the rule curves so that water during normal operational periods of the reservoir is held back and used to meet the demand during extreme low flow periods. This study is continuing to develop such hedging-integrated rule curves.

Acknowledgement

The work reported here was funded by the UK-NERC (Project NE/1022337/1) – Mitigating Climate Change impacts on India Agriculture through Improved Irrigation Water Management (MICCI) – as part of the Changing Water Cycle (South Asia Thematic Programme).

References

Adeloye A.J., Rustum R. and Ibrahim D.K. (2011). Kohonen self-organizing map estimator for the reference crop evapotranspiration. *Water Resources Re*search 47(W08523): 1-19.

Adeloye, A.J. (2012) Hydrological sizing of water supply reservoir. In (Bengtsson, L, Herschy, RW, and Fairbridge, RW (eds.)) *Encyclopedia of lakes and reservoirs*, Springer, Dordrecht, 346-355

Fiering M.B. (1982). Estimates of resilience indices by simulation. Water Resources Research, 18(1), 41 – 50.

Hossain M.S. and El-shafie A. (2013). Intelligent systems in optimizing reservoir operation policy: a review. *Water Resources Management* 27: 3387-3407

Jain S.K., Agarwal P.K. and Singh V.P. (2007). *Hydrology and water resources of India*, Springer, The Netherlands.

McMahon T.A. and Adeloye A.J. (2005). Water Resources Yield. Water Resources Publications, Littleton, CO, USA.

McMahon T.A., Adeloye A.J. and Zhou S.L. (2006). Understanding performance measures of reservoirs, *Journal of Hydrology*. 324: 359-382.

Murphy C. Fealy R. Charlton R. and Sweeney J.S. (2006). The reliability of an "off the shelf" conceptual rainfall-runoff model for use in climate impact assessment: uncertainty quantification using Latin Hypercube Sampling. *Area* 38(1): 65-78.

Nawaz N.R. and Adeloye A.J. (2006). Monte Carlo assessment of sampling uncertainty of climate change impacts on water resources yield in Yorkshire, England. *Climatic Change* 78: 257-292.

Pilling C. and Jones J.A. (1999). High resolution climate change scenarios: implications for British runoff. *Hydrological Processes* 13(17): 2877–2895.

Sandoval-Soils S., Mckinney D.C. and Loucks D.P. (2011). Sustainability index for water resources planning and management. *Journal of Water Resources Planning and Management (ASCE)* 137(5): 381-389.

Wardlaw R. and Sharif M. (1999). Evaluation of genetic algorithms for optimal reservoir operation. *Journal of Water Resources Planning and Management (ASCE)* 125: 25-33.